

On a Klein-Gordon Reduction for Oscillons

Atanas G. Stefanov and Milena Stanislavova

*Department of Mathematics, University of Alabama - Birmingham,
1402 10th Avenue South, Birmingham AL 35294, USA*

Jesús Cuevas-Maraver

*Grupo de Física No Lineal, Departamento de Física Aplicada I,
Universidad de Sevilla, Escuela Politécnica Superior,
C/ Virgen de África, 7, 41011 Sevilla, Spain and
Instituto de Matemáticas de la Universidad de Sevilla (IMUS),
Edificio Celestino Mutis, Avda. Reina Mercedes s/n, 41012 Sevilla, Spain*

Panayotis G. Kevrekidis

*Department of Mathematics and Statistics, University of Massachusetts, Amherst, Massachusetts 01003-4515, USA and
Department of Physics, University of Massachusetts, Amherst, Massachusetts 01003, USA*

In the present work we examine the dynamics of a model for oscillons in 1-dimensional space-time field theories with a cubic nonlinearity. We utilize a reduction of the model to first and third harmonics, which leads to a reduced partial differential equation (PDE) system whose steady states are candidates for the original PDE oscillons. We analyze the steady states of this model and their stability, including via tools such as index theory. We develop suitable functionals needed for the study of such stationary states, as well as an analogue of the famous Vakhitov-Kolokolov criterion for a quantity whose change of monotonicity reflects a change of stability. Then, we test the relevant predictions, over the full range of oscillon frequencies, through systematic numerical computations of both the reduced model, its steady states and stability, and also of the original PDE model, identifying its time-periodic oscillon solution. Our results yield some significant connections with previous studies, but also some fundamental new insights both on the reduced system and the dynamics of the original system.

I. INTRODUCTION

The study of oscillons is a topic of wide interest, notably in the context of cosmological models and their inflationary dynamics [1]. Such solutions have appeared in the context of Einstein-Klein-Gordon equations [2], in the study of the dynamics of strings [3], as well as in the analysis and computation of electroweak interactions [4, 5]. The relevant states have also been shown to be of interest in the context of two-dimensional models of the Abelian-Higgs type [6]. In such settings, they have also been spontaneously detected, e.g., as remnants of vortex-antivortex annihilations [7]. Finally, they have been argued to be relevant to three-dimensional variants of the famous ϕ^4 -model [7]. Indeed, they generally constitute a pillar of solitonic features of relevance to a wide range of models in areas of field theory and cosmology [8–11]. It is worth noting here also that in other settings including dissipative systems and most notably vibrating granular beds [12], oscillon waveforms have been observed experimentally [13].

A significant number of studies has focused on the classic ϕ^4 oscillon [14], which lives on top of a unit background. Yet, a variant of the problem that possesses interesting dynamical features is that with the “flipped sign” of the nonlinearity, as considered, e.g., early on by Kosevich and Kovalev in [15]. The latter model has a vanishing field as the stable homogeneous equilibrium on top of which the oscillon lives. The model is also rather nontrivial to analytically study, among other reasons, due to its potential blow up singularity features [16]. In a recent development, the work of [17] provided a systematic approach towards the needed multiple scale nature of a variational formalism, so as to capture the proper collective coordinate dynamical description of the oscillon and its potential regime of dynamical stability. Another key recent study identified the diagram of the energy vs. frequency of the oscillon structures, albeit in the regular ϕ^4 model in the work of [18].

In the present work, we take a complementary approach to the ones utilized so far, as a method that can be applied to this problem, but also could be of interest to other settings with spatially localized, temporally periodic solutions. In particular, in the spirit of a few mode Galerkin approach, we decompose the solution into the fundamental mode and its third harmonic (due to the nature of our nonlinearity) and truncate higher order modes. In this way, and ascribing spatio-temporal dependence, aiming to capture the spatial dependence and the slow temporal dynamics, we provide a methodology that can be used to obtain meaningful trial solutions towards the full problem. I.e., while the full problem may have “breather-type” solutions [19, 20], we aim to approximate these as steady state (localized) spatial profiles multiplying the first and third harmonics, while the implicit assumption is that higher order terms may be small for this approximation to be meaningful.

In what follows, we will first analyze the resulting partial differential equation (PDE) models for the prefactor terms of the first and third harmonic. We will bring to bear tools from PDEs and dynamical systems to provide information for the steady states of the resulting model and its stability. In the process, we will devise suitable Lyapunov-like functionals that will provide stability information regarding their extremizing states, and we will obtain a Vakhitov-Kolokolov [21]-type criterion for this system, involving a suitable frequency-weighted variant of the mass of the two modes, whose change of monotonicity will reflect a change in stability. The use of index theory will provide a systematic tool for the identification of the spectral stability of the different states that will be uncovered. Subsequently, this detailed information will be tested in numerical computations. The different states will be numerically identified and continued as a function of the mode frequency. We will see that the few-mode reduction has some remarkable successes and also some notable shortcomings in capturing the full time-periodic oscillon states. We believe that this analysis offers a valuable PDE tool in the arsenal of the applied scientist towards obtaining and testing information, not only for oscillon but also for more general such time-periodic, spatially localized states.

Our presentation will be structured as follows. In section II we will present the model setup. In section III we provide some basic mathematical background results, while in section IV we construct the waves. Their stability is examined in section V. Section VI contains our numerical results, while section VII summarizes our findings and provides some directions for future study.

II. MODEL SETUP

We would like to study the following Klein-Gordon system, [17]

$$z_{tt} - z_{xx} + 4z - 2z^3 = 0, (t, x) \in \mathbb{R}_+ \times \mathbb{R}. \quad (\text{II.1})$$

As is well-known, such a system is Hamiltonian, with

$$H[z] = \frac{1}{2} \int z_x^2 + z_t^2 + 4z^2 - \frac{1}{2}z^4 dx. \quad (\text{II.2})$$

Specifically, we are interested in the oscillons, which are real-valued, time-periodic *approximate solutions* of the form

$$z = u(t, x)e^{i\omega t} + \bar{u}(t, x)e^{-i\omega t} + v(t, x)e^{3i\omega t} + \bar{v}(t, x)e^{-3i\omega t} \quad (\text{II.3})$$

In particular, we plug the ansatz (II.3) into the KG equation (II.1), and we equate the terms containing $e^{i\omega t}, e^{3i\omega t}$ (i.e. we ignore higher order time harmonics $e^{\pm 5i\omega t}, e^{\pm 7i\omega t}, e^{\pm 9i\omega t}$). The resulting system is the following approximate, coupled Klein-Gordon system, in the form

$$\begin{cases} u_{tt} + 2i\omega u_t - u_{xx} + (4 - \omega^2)u - (6u^2\bar{u} + 6\bar{u}^2v + 12u|v|^2) = 0 \\ v_{tt} + 6i\omega v_t - v_{xx} + (4 - 9\omega^2)v - (2u^3 + 12|u|^2v + 6|v|^2v) = 0. \end{cases} \quad (\text{II.4})$$

Now, we are interested in time independent [22] solutions of this system $(u, v) = (\phi, \psi)$, which satisfy the elliptic system

$$\begin{cases} -\phi'' + (4 - \omega^2)\phi - (6\phi^2\bar{\phi} + 6\bar{\phi}^2\psi + 12\phi|\psi|^2) = 0, \\ -\psi'' + (4 - 9\omega^2)\psi - (2\phi^3 + 12|\phi|^2\psi + 6|\psi|^2\psi) = 0. \end{cases} \quad (\text{II.5})$$

We are looking for real-valued solutions ϕ, ψ of (II.5). In such a case, the approximate solution (II.3) is in the form

$$2[\phi \cos(\omega t) + \psi \cos(3\omega t)]. \quad (\text{II.6})$$

From this point on, our object of interest is the dynamics of the system (II.4), specifically the stability of its stationary solutions (ϕ, ψ) of (II.5).

Theorem II.1 (Existence of bell-shaped oscillons). *Let $|\omega| < \frac{2}{3}$. Then, the system (II.5) has a solution (ϕ, ψ) , where both ϕ, ψ are real-valued and bell-shaped functions [23]. In addition, ϕ, ψ are smooth and exponentially localized. More specifically,*

$$\phi(x) \sim e^{-\sqrt{4-\omega^2}|x|}, \quad \psi(x) \sim e^{-\sqrt{4-9\omega^2}|x|}, |x| \gg 1.$$

A. Linearization around the steady states

Let us now consider the linearized problem associated with the system (II.4). To this end, we adopt the variables

$$u = \phi + p + iq, v = \psi + r + is$$

Plugging this ansatz in (II.4), taking real and imaginary parts separate and ignoring all quadratic and higher order terms leads to

$$\begin{cases} p_{tt} - 2\omega q_t - p_{xx} + (4 - \omega^2)p - [(18\phi^2 + 12\psi^2 + 12\phi\psi)p + (6\phi^2 + 24\phi\psi)r] = 0 \\ q_{tt} + 2\omega p_t - q_{xx} + (4 - \omega^2)q - [(6\phi^2 + 12\psi^2 - 12\phi\psi)q + 6\phi^2s] = 0 \\ r_{tt} - 6\omega s_t - r_{xx} + (4 - 9\omega^2)r - [(12\phi^2 + 18\psi^2)r + (6\phi^2 + 24\psi^2)p] = 0 \\ s_{tt} + 6\omega r_t - s_{xx} + (4 - 9\omega^2)s - [6\phi^2q + (12\phi^2 + 6\psi^2)s] = 0. \end{cases} \quad (\text{II.7})$$

This is the form of the linearized problem. We now need to convert this to a more standard, first order in time, eigenvalue problem. This is done in a number of steps.

1. The eigenvalue problem

In matrix form,

$$\begin{pmatrix} p \\ q \\ r \\ s \end{pmatrix}_{tt} + \begin{pmatrix} 0 & -2\omega & 0 & 0 \\ 2\omega & 0 & 0 & 0 \\ 0 & 0 & 0 & -6\omega \\ 0 & 0 & 6\omega & 0 \end{pmatrix} \begin{pmatrix} p \\ q \\ r \\ s \end{pmatrix}_t + \mathcal{H} \begin{pmatrix} p \\ q \\ r \\ s \end{pmatrix}_t = 0, \quad (\text{II.8})$$

where

$$\mathcal{H} := \begin{pmatrix} \mathcal{H}_1 & 0 & -24\phi\psi - 6\phi^2 & 0 \\ 0 & \mathcal{H}_2 & 0 & -6\phi^2 \\ -24\phi\psi - 6\phi^2 & 0 & \mathcal{H}_3 & 0 \\ 0 & -6\phi^2 & 0 & \mathcal{H}_4 \end{pmatrix} \quad (\text{II.9})$$

and

$$\begin{aligned} \mathcal{H}_1 &= -\partial_{xx} + (4 - \omega^2) - 18\phi^2 - 12\psi^2 - 12\phi\psi; & \mathcal{H}_2 &= -\partial_{xx} + (4 - \omega^2) - 6\phi^2 - 12\psi^2 + 12\phi\psi \\ \mathcal{H}_3 &= -\partial_{xx} + (4 - 9\omega^2) - 12\phi^2 - 18\psi^2; & \mathcal{H}_4 &= -\partial_{xx} + (4 - 9\omega^2) - 12\phi^2 - 6\psi^2 \end{aligned}$$

Note that the operator \mathcal{H} is self-adjoint, for nice enough ϕ, ψ , when taken with the domain $H^2(\mathbb{R}) \times H^2(\mathbb{R}) \times H^2(\mathbb{R}) \times H^2(\mathbb{R})$, while

$$\mathcal{J} := \begin{pmatrix} 0 & -2\omega & 0 & 0 \\ 2\omega & 0 & 0 & 0 \\ 0 & 0 & 0 & -6\omega \\ 0 & 0 & 6\omega & 0 \end{pmatrix},$$

is skew-symmetric, i.e. $\mathcal{J}^* = -\mathcal{J}$. The corresponding eigenvalue problem, which can be obtained by the assignment

$$\begin{pmatrix} p \\ q \\ r \\ s \end{pmatrix} \rightarrow e^{\lambda t} \begin{pmatrix} p \\ q \\ r \\ s \end{pmatrix} =: e^{\lambda t} \vec{z}$$

can be written in the form

$$\lambda^2 \vec{z} + \lambda \mathcal{J} \vec{z} + \mathcal{H} \vec{z} = 0.$$

This eigenvalue problem is a pencil of order two, and these have been an object of intense investigations. A standard equivalence in a more classical Hamiltonian form is as follows[24]

$$\begin{pmatrix} 0 & -Id \\ Id & -\mathcal{J} \end{pmatrix} \begin{pmatrix} \mathcal{H} & 0 \\ 0 & I \end{pmatrix} \begin{pmatrix} \vec{z} \\ \vec{w} \end{pmatrix} = \lambda \begin{pmatrix} \vec{z} \\ \vec{w} \end{pmatrix} \quad (\text{II.10})$$

This prompts the following definition.

Definition II.2. *We say that the steady state solution (ϕ, ψ) of (II.5) is spectrally stable, if the eigenvalue problem (II.10) does not have non-trivial solutions with $\text{Re}\lambda > 0, \vec{z} \neq 0$*

B. Stability of the waves

Next, we address the important issue of symmetries and the corresponding eigenvalues at zero for the linearized problem, that arise.

1. Symmetries of the system

We can identify at least two symmetries of the system (II.5), namely a translational and (phase) modulational invariance. Specifically, for every solution (ϕ, ψ) of (II.5) and arbitrary real y , then $(\phi(\cdot - y), \psi(\cdot - y))$, $(e^{iy}\phi, e^{3iy}\psi)$ are solutions as well. The usual differentiation in the parameter y , and taking into account the setup of \mathcal{H} , provides two elements in $\text{Ker}[\mathcal{H}]$. More concretely,

$$\begin{pmatrix} \phi' \\ 0 \\ \psi' \\ 0 \end{pmatrix}, \quad \begin{pmatrix} 0 \\ \phi \\ 0 \\ 3\psi \end{pmatrix} \in \text{Ker}[\mathcal{H}].$$

2. Non-degeneracy of the wave pair (ϕ, ψ)

We now introduce the notion of a non-degeneracy for the wave pair (ϕ, ψ) .

Definition II.3. *We say that the solution (ϕ, ψ) is non-degenerate, if there are no more elements of $\text{Ker}[\mathcal{H}]$ other than those already found. Specifically,*

$$\text{Ker}[\mathcal{H}] = \text{span} \left[\begin{pmatrix} \phi' \\ 0 \\ \psi' \\ 0 \end{pmatrix}, \quad \begin{pmatrix} 0 \\ \phi \\ 0 \\ 3\psi \end{pmatrix} \right]$$

In other words, non-degeneracy means that the only zeros in the kernel of \mathcal{H} are those generated by the symmetries of the system.

We are now ready to state the main stability result.

Theorem II.4. *Let $\omega : |\omega| < \frac{2}{3}$. Assume that the steady state solution (ϕ, ψ) of (II.4), constructed in Theorem II.1, is a non-degenerate, smooth function of ω . That is, the mapping $\omega \rightarrow (\phi, \psi)$ is Frechet differentiable.*

Then, it is spectrally stable if and only if the following holds true

$$\omega \partial_\omega \int_{\mathbb{R}} (\phi^2 + 9\psi^2) dx + \int_{\mathbb{R}} (\phi^2 + 9\psi^2) dx < 0.$$

Equivalently, $\omega \rightarrow \omega \int_{\mathbb{R}} (\phi^2 + 9\psi^2) dx$ is decreasing.

III. PRELIMINARIES

We use standard notations for the L^p spaces, namely with the norm $\|f\|_p := \left(\int_{\mathbb{R}} |f(x)|^p dx \right)^{1/p}$, and the Sobolev spaces $H^s(\mathbb{R})$. The Sobolev embedding guarantees that for all $2 < p < \infty$, there is a constant C_p , so that $\|u\|_p \leq C_p \|u\|_{H^1}$.

A. Decreasing rearrangements and compactness criteria

One tool that will be useful in the sequel is the notion of the decreasing rearrangement. For a function $f : \mathbb{R} \rightarrow \mathbb{R}$, there exists an even, positive, non-increasing on $(0, +\infty)$ function f^* , so that the corresponding level functions coincide, i.e., $d_f(\alpha) = \{x : |f(x)| > \alpha\} = \{x : f^*(x) > \alpha\} = d_{f^*}(\alpha)$. Alternatively, a constructive definition may be given as follows

$$f^*(t) = \inf \{s : d_f(s) \leq 2|t|\}, \quad t \in \mathbb{R}$$

Either way, we conclude that $\|f\|_p = \|f^*\|_p$. Additionally, there are the standard inequalities

$$\int_{\mathbb{R}} f(x)g(x)dx \leq \int_{\mathbb{R}} f^*(x)g^*(x)dx, \int_{\mathbb{R}^2} f(x-y)g(y)h(x)dxdy \leq \int_{\mathbb{R}^2} f^*(x-y)g^*(y)h^*(x)dxdy$$

The Szegö inequality guarantees that $f^* \in H^1$, whenever $f \in H^1(\mathbb{R})$ and moreover,

$$\|\partial_x f\| \geq \|\partial_x f^*\| \quad (\text{III.1})$$

In case of equality in (III.1), one concludes that the function f coincides with its rearrangement, i.e. $f = f^*$, and therefore it belongs to a class of functions, usually referred to as bell-shaped.

The Riesz-Relich-Kolmogorov compactness criteria (or rather a consequence thereof), is the following - a sequence $\{u_n\}_n$ is compact in $L^p(\mathbb{R})$, $1 < p < \infty$, if

- $\sup_n \|u_n\|_{H^1(\mathbb{R})} < \infty$
- For every $\epsilon > 0$, there exists $R = R_\epsilon > 0$, so that

$$\sup_n \int_{|x| > R} |u_n(x)|^p dx < \epsilon.$$

B. Basics of the instability index theory

Consider a Hamiltonian eigenvalue problem in the form

$$JLu = \lambda u \quad (\text{III.2})$$

where $J^* = -J$ and $L^* = L$, with appropriate domains for the composition operator JL . Assume in addition that both J, L act on spaces of functions, and they do preserve real-valued functions. The stability for (III.2) is a fundamental problem in the modern dynamics. Specifically, as in Definition II.2, we say that the problem (III.2) is stable, if there are no non-trivial solutions of (III.2) with $\text{Re}\lambda > 0$. In order to introduce some relevant notions, we assume that L is semi-bounded from below, that is there exists a constant C , so that $L \geq C$ in the sense of quadratic forms. In fact, we assume that its negative subspace X_- is finite dimensional and $P_{X_-} LP_{X_-}$ has only point spectrum, each with finite multiplicity. Denote its Morse index by

$$n(L) = \dim[X_-] = \#\{\sigma : \sigma < 0 : \sigma \in \sigma_{p.p.}(L)\}.$$

Next, let k_r be the number of positive eigenvalues of (III.2), k_c be the number of quadruplets of eigenvalues with non-zero real and imaginary parts, and k_i^- , the number of pairs of purely imaginary eigenvalues with negative Krein-signature. For a simple pair of imaginary eigenvalues $\pm i\mu$, $\mu \neq 0$, and the corresponding eigenvector $\vec{h} = \begin{pmatrix} h_1 \\ h_2 \end{pmatrix}$, the Krein signature, either ± 1 is the following quantity $\text{sgn}(\langle \mathcal{L}\vec{h}, \vec{h} \rangle)$. Consider the generalized kernel of JL

$$gKer(JL) = \text{span}[(Ker(JL))^l, l = 1, 2, \dots].$$

Assume that $\dim(gKer(JL)) < \infty$, although this is, strictly speaking, not required in [25]. Select a basis in

$$gKer(JL) \ominus Ker(L) = \text{span}[\eta_j, j = 1, \dots, N].$$

Introduce $\mathcal{D} \in \mathcal{M}_{N \times N}$,

$$\mathcal{D} := \{\mathcal{D}_{ij}\}_{i,j=1}^N : \mathcal{D}_{ij} = \langle \mathcal{L}\eta_i, \eta_j \rangle.$$

Then, following [25], we have the following formula, relating the number of “instabilities” or Hamiltonian index of the eigenvalue problem (III.2) and the Morse indices of the operators L and \mathcal{D} ,

$$k_{Ham} := k_r + 2k_c + 2k_i^- = n(L) - n(\mathcal{D}). \quad (\text{III.3})$$

Specifically, if $n(L) = 1$, it follows from (III.3) that $k_c = k_i^- = 0$ and

$$k_r = 1 - n(\mathcal{D}). \quad (\text{III.4})$$

Note that in the case $n(L) = 1$, instability occurs exactly when $n(\mathcal{D}) = 0$, while stability occurs whenever $n(\mathcal{D}) = 1$. We formulate this in a corollary as follows.

Corollary III.1. *Assume that in the eigenvalue problem (III.2), we have that $n(L) = 1$. Then, the problem (III.2) is spectrally stable if and only if $n(\mathcal{D}) = 1$.*

IV. CONSTRUCTION OF THE WAVES

We can clearly see that the elliptic system (II.5) is of the form

$$\begin{cases} -\phi'' + (4 - \omega^2)\phi - \frac{\partial F}{\partial \phi} = 0 \\ -\psi'' + (4 - 9\omega^2)\psi - \frac{\partial F}{\partial \psi} = 0 \end{cases} \quad (\text{IV.1})$$

where

$$F(u, v, \bar{u}, \bar{v}) = 3|u|^4 + 2\bar{u}^3v + 12|u|^2|v|^2 + 2u^3\bar{v} + 3|v|^4 = 3(|u|^4 + |v|^4 + 4|u|^2|v|^2) + 4\text{Re}\bar{u}^3v. \quad (\text{IV.2})$$

As such, it supports a Hamiltonian structure in the form

$$H_1[\phi, \psi] = \frac{1}{2} \int |\phi'|^2 + |\psi'|^2 + (4 - \omega^2)|\phi|^2 + (4 - 9\omega^2)|\psi|^2 + 6(|\phi|^4 + |\psi|^4 + 4|\phi|^2|\psi|^2) + 8\text{Re}[\bar{\phi}^3\psi]dx \quad (\text{IV.3})$$

Clearly, one obtains $H_1[\phi, \psi] = H[z]$, under the transformation (II.6). While here we mention in passing the Hamiltonian structure of the steady state ODEs, naturally, the relevant transformation can also be used to obtain the Hamiltonian structure of the PDEs of the system of Eqs. (II.4).

Proposition IV.1. *Let $|\omega| < \frac{2}{3}$. Then, the variational problem*

$$\begin{cases} J[u, v] = \int_{-\infty}^{+\infty} 3(|u|^4 + |v|^4 + 4|u|^2|v|^2) + 4\text{Re}\bar{u}^3v \rightarrow \max \\ I[u, v] = \int_{-\infty}^{+\infty} (u')^2 + (v')^2 + (4 - \omega^2)u^2 + (4 - 9\omega^2)v^2 dx = 1. \end{cases} \quad (\text{IV.4})$$

has a solution (U, V) , with $U \geq 0, V \geq 0$, and U, V are both even. In addition, (U, V) satisfy the Euler-Lagrange equation,

$$\begin{cases} -U'' + (4 - \omega^2)U - \frac{1}{J_0}(6U^3 + 12V^2U + 6U^2V) = 0, \\ -V'' + (4 - 9\omega^2)V - \frac{1}{J_0}(6V^3 + 12U^2V + 2U^3) = 0. \end{cases} \quad (\text{IV.5})$$

where we denoted $J_0 := \sup_{I[u, v]=1} J[u, v] = J[U, V]$.

Remark:

- The solutions (ϕ, ψ) of (IV.1) may be obtained as $\phi = c_0U, \psi = c_0V$, where c_0 depends only on $J[U, V]$, and so on ω only.
- One concern is that for some values of $\omega, 0 < \frac{2}{3} - |\omega| << 1$ (namely the ones for which $4 - 9\omega^2$ is sufficiently small), we may get the “semi-simple” solution $U = 0, V = C\text{sech}(\sqrt{4 - 9\omega^2}x)$ (for suitably chosen C , so that $I[0, V] = 1$). This would be a minimizer of (IV.4) anyway, but trivial. We check numerically, see Fig. 3 below, that this indeed happens for $0.5316 < \omega < 2/3$.

Proof. The proof is rather straightforward. To this end, note that by Sobolev embedding $\|u\|_4 \leq C\|u\|_{H^1}$. Estimating $J[u, v]$ by Hölder’s, we see that

$$J[u, v] \leq C(\|u\|_4^4 + \|v\|_4^4) \leq C\|u\|_{H^1}^4 + \|v\|_{H^1}^4 \leq CI^2[u, v].$$

It follows that $J[u, v]$ is bounded from above, when u, v are under the constraint $I[u, v] = 1$. Moreover, by elementary properties of the decreasing rearrangements, we have that

$$\begin{aligned} J[u, v] &= \int_{-\infty}^{+\infty} 3(|u|^4 + |v|^4 + 4|u|^2|v|^2) + 4\text{Re}\bar{u}^3v \leq \\ &\leq \int_{-\infty}^{+\infty} 3(|u^*|^4 + |v^*|^4 + 4|u^*|^2|v^*|^2) + 4(u^*)^3v^* = J[u^*, v^*]. \end{aligned}$$

In terms of the constraints, using the Szegö inequality, we have

$$I[u, v] \geq I[u^*, v^*].$$

Assuming for a moment that there holds the strict inequality, $1 = I[u, v] > I[u^*, v^*]$, say $I[u^*, v^*] = a < 1$, we arrive at a contradiction, since then u^*, v^* satisfy

$$\begin{cases} J[u^*, v^*] \geq J[u, v] \\ I[u^*, v^*] = a < 1 \end{cases}$$

But since the problem is scale invariant, we have that $I[a^{-1/2}u^*, a^{-1/2}v^*] = 1$ satisfy the original constraint, while

$$J[a^{-1/2}u^*, a^{-1/2}v^*] = a^{-2}J[u^*, v^*] \geq a^{-2}J[u, v] > J[u, v],$$

in clear contradiction with the setup of the variational problem (IV.4). So, $I[u, v] = I[u^*, v^*]$, whence it follows that $u = u^*, v = v^*$, i.e., the variational problem may be taken to maximize J only on the set of bell-shaped functions. Using the properties of the bell-shaped functions, and the constraint we have that

$$u^2(x) \leq \frac{1}{2x} \int_{-x}^x u^2(y) dy \leq \frac{1}{2x} \|u\|^2 \leq \frac{C_\omega}{x}.$$

and similar for v . It follows that, for every $R > 0$,

$$\int_{|x|>R} u^4(x) dx \leq C \int_{|x|>R} x^{-2} dx \leq CR^{-1},$$

and similar for v . This, together with the constraint $\|u\|_{H^1} + \|v\|_{H^1} \leq C$, implies by the Riesz-Kolmogorov criteria, that any maximizing sequence for (IV.4) is in fact compact in $L^4(\mathbb{R})$. Thus, starting with a maximizing sequence for (IV.4), i.e.

$$I[u_n, v_n] = 1, J[u_n, v_n] \rightarrow \sup_{I[u, v]=1} J[u, v]$$

and after taking a strongly convergent in L^4 , subsequence $\lim_n \|u_n - U\|_4 = 0, \lim_n \|v_n - V\|_4 = 0$, whence

$$\lim_n J[u_n, v_n] = J[U, V].$$

At the same time, by the lower semi-continuity of the H^1 norms (with respect to weak convergence, so certainly with respect to L^4 convergence),

$$I[U, V] \leq \liminf_n I[u_n, v_n] = 1.$$

If in fact, we assume that $I[U, V] < 1$, we obtain the same contradiction as above (the value of $\sup_{I[u, v]=1} J[u, v]$ is bigger than it can possibly be), so it follows that $I[U, V] = 1$ (and in fact, one may conclude from this that even stronger convergence holds, namely $\lim_n \|u_n - U\|_{H^1} = 0, \lim_n \|v_n - V\|_{H^1} = 0$).

We now derive the Euler-Lagrange equations. Taking $U + \epsilon h_1, V + \epsilon h_2$ for some testing functions h_1, h_2 , we have that the following scalar function achieves a maximum at $\epsilon = 0$,

$$g(\epsilon) = \frac{J[U + \epsilon h_1, V + \epsilon h_2]}{I^2[U + \epsilon h_1, V + \epsilon h_2]}$$

It follows that $g'(0) = 0$, while $g''(0) \leq 0$. Note $J_0 > 0$. We have

$$\begin{aligned} & J[U + \epsilon h_1, V + \epsilon h_2] = J_0 + \\ & + \epsilon (12\langle U^3, h_1 \rangle + 12\langle V^3, h_2 \rangle + 24\langle V^2 U, h_1 \rangle + 24\langle U^2 V, h_2 \rangle + 12\langle U^2 V, h_1 \rangle + 4\langle U^3, h_2 \rangle) + O(\epsilon^2) \\ & I^2[U + \epsilon h_1, V + \epsilon h_2] = 1 + 2\epsilon (\langle -U'' + (4 - \omega^2)U, h_1 \rangle + \langle -V'' + (4 - \omega^2)V, h_2 \rangle) + O(\epsilon^2). \end{aligned}$$

Writing out the first order in ϵ terms, arising in $g(\epsilon)$ leads to the formulas

$$\begin{aligned} & 12\langle U^3, h_1 \rangle + 12\langle V^3, h_2 \rangle + 24\langle V^2 U, h_1 \rangle + 24\langle U^2 V, h_2 \rangle + 12\langle U^2 V, h_1 \rangle + 4\langle U^3, h_2 \rangle = \\ & = 2J_0 (\langle -U'' + (4 - \omega^2)U, h_1 \rangle + \langle -V'' + (4 - \omega^2)V, h_2 \rangle). \end{aligned}$$

Since h_1, h_2 are independent increments, we have that U, V are weak solutions of the elliptic system (IV.5). Standard elliptic estimates for (IV.5) imply that such solutions are in fact $H^\infty(\mathbb{R})$, so in particular U, V are $C^\infty(\mathbb{R})$ functions. In addition, the large x asymptotics for U, V are as follows

$$U(x) \sim e^{-\sqrt{4-\omega^2}|x|}, V(x) \sim e^{-\sqrt{4-9\omega^2}|x|}.$$

We now pass to the second order expansion, in terms of ϵ , for the function g . To simplify matters, we work with the additional restriction that the increments (h_1, h_2) satisfy the constraint,

$$\operatorname{Re}[\langle -U'' + (4 - \omega^2)U, h_1 \rangle + \langle -V'' + (4 - \omega^2)V, h_2 \rangle] = 0. \quad (\text{IV.6})$$

As a consequence of this extra property, we have that

$$I^2[U + \epsilon h_1, V + \epsilon h_2] = 1 + \epsilon^2(\|h'_1\|^2 + \|h'_2\|^2 + (4 - \omega^2)\|h_1\|^2 + (4 - 9\omega^2)\|h_2\|^2). \quad (\text{IV.7})$$

Next, we find the second order expansion, in terms of ϵ , for the functional $J[U + \epsilon h_1, V + \epsilon h_2]$. We have

$$J[U + \epsilon h_1, V + \epsilon h_2] = J_0 + \epsilon(A_1[h_1] + A_2[h_2] + A_3[\bar{h}_1] + A_4[\bar{h}_2]) + \epsilon^2 B[h_1, h_2, \bar{h}_1, \bar{h}_2] + O(\epsilon^3),$$

where A_1, \dots, A_4 are linear forms [26], while

$$\begin{aligned} B[h_1, h_2, \bar{h}_1, \bar{h}_2] &= \int (12U^2 h_1 \bar{h}_1 + 3U^2(h_1^2 + \bar{h}_1^2) + 12V^2 h_2 \bar{h}_2 + 3V^2(h_2^2 + \bar{h}_2^2)) + \\ &+ \int (12UV(h_1 + \bar{h}_1)(h_2 + \bar{h}_2) + 12U^2 h_2 \bar{h}_2 + 12V^2 h_1 \bar{h}_1) + \\ &+ \int (6U^2(\bar{h}_1 h_2 + \bar{h}_2 h_1) + 6UV(\bar{h}_1^2 + h_1^2)). \end{aligned}$$

As a consequence of the expansion for B and (IV.7), we have that

$$0 \geq g''(0) = 2(B[h_1, h_2, \bar{h}_1, \bar{h}_2] - J_0(\|h'_1\|^2 + \|h'_2\|^2 + (4 - \omega^2)\|h_1\|^2 + (4 - 9\omega^2)\|h_2\|^2)). \quad (\text{IV.8})$$

It is technically more convenient to pass to the new variables $h_1 = p + iq, h_2 = r + is$, so that we can rewrite (IV.8) as follows

$$\begin{aligned} &\|p'\|^2 + \|q'\|^2 + \|r'\|^2 + \|s'\|^2 + (4 - \omega^2)(\|p\|^2 + \|q\|^2) + (4 - 9\omega^2)(\|r\|^2 + \|s\|^2) \geq \\ &\geq \frac{1}{J_0} \int (12U^2(p^2 + q^2) + 6U^2(p^2 - q^2) + 12V^2(r^2 + s^2) + 6V^2(r^2 - s^2)) + \\ &+ \frac{12}{J_0} \int (4UVpr + U^2(r^2 + s^2) + V^2(p^2 + q^2)) + \\ &+ \frac{12}{J_0} \int (U^2(pr + qs) + UV(p^2 - q^2)). \end{aligned}$$

This last inequality should hold for all increments $(p + iq, r + is)$ satisfying (IV.6), which is equivalent to

$$\begin{pmatrix} p \\ q \\ r \\ s \end{pmatrix} \perp \begin{pmatrix} -U'' + (4 - \omega^2)U \\ 0 \\ -V'' + (4 - 9\omega^2)V \\ 0 \end{pmatrix} \quad (\text{IV.9})$$

The condition $g''(0) \leq 0$ may be expressed equivalently as the positivity of the following self-adjoint operator, on the co-dimension one subspace described by (IV.9),

$$\mathcal{L} := \begin{pmatrix} \mathcal{L}_1 & 0 & -\frac{24}{J_0}UV - \frac{6}{J_0}U^2 & 0 \\ 0 & \mathcal{L}_2 & 0 & -\frac{6}{J_0}U^2 \\ -\frac{24}{J_0}UV - \frac{6}{J_0}U^2 & 0 & \mathcal{L}_3 & 0 \\ 0 & -\frac{6}{J_0}U^2 & 0 & \mathcal{L}_4 \end{pmatrix}$$

where

$$\begin{aligned} \mathcal{L}_1 &:= -\partial_{xx} + (4 - \omega^2) - \frac{18}{J_0}U^2 - \frac{12}{J_0}V^2 - \frac{12}{J_0}UV \\ \mathcal{L}_2 &:= -\partial_{xx} + (4 - \omega^2) - \frac{6}{J_0}U^2 - \frac{12}{J_0}V^2 + \frac{12}{J_0}UV \\ \mathcal{L}_3 &:= -\partial_{xx} + (4 - 9\omega^2) - \frac{18}{J_0}V^2 - \frac{12}{J_0}U^2 \\ \mathcal{L}_4 &:= -\partial_{xx} + (4 - 9\omega^2) - \frac{6}{J_0}V^2 - \frac{12}{J_0}U^2 \end{aligned}$$

□

Clearly, the assignment

$$\phi := \frac{U}{\sqrt{J_0}}, \psi := \frac{V}{\sqrt{J_0}} \quad (\text{IV.10})$$

produces bell-shaped solutions of (II.5), moreover one can infer spectral properties of the corresponding operator, from the properties of the operator \mathcal{L} . In fact, we have established more, namely that $\langle \mathcal{L}h, h \rangle \geq 0$, whenever $h \perp \begin{pmatrix} -U'' + (4 - \omega^2)U \\ 0 \\ -V'' + (4 - 9\omega^2)V \\ 0 \end{pmatrix}$. Using the rescaling transformation (IV.10), this is equivalent to

$$\langle \mathcal{H}u, u \rangle \geq 0, u \perp \begin{pmatrix} -\phi'' + (4 - \omega^2)\phi \\ 0 \\ -\psi'' + (4 - 9\omega^2)\psi \\ 0 \end{pmatrix} \quad (\text{IV.11})$$

We state the results in the following corollary.

Corollary IV.2. *The linearized self-adjoint operator operator \mathcal{H} , introduced in (II.9), has exactly one negative eigenvalue, i.e., the property $n(\mathcal{H}) = 1$.*

V. STABILITY OF THE WAVES

In this section, we consider the eigenvalue problem (II.10). Since the self-adjoint portion of it has the property

$$n \begin{pmatrix} \mathcal{H} & 0 \\ 0 & I \end{pmatrix} = n(\mathcal{H}) = 1,$$

according to Corollary IV.2, we can apply the formula (III.4). To this end, we need to calculate the generalized kernel $gKer(\begin{pmatrix} 0 & -I \\ I & -\mathcal{J} \end{pmatrix} \begin{pmatrix} \mathcal{H} & 0 \\ 0 & I \end{pmatrix})$, compute the matrix \mathcal{D} and then $n(\mathcal{D})$.

It is actually easy to see that for this program, we may as well restrict our attention to the subspace of even functions. Indeed, the eigenvalue problem (II.10) splits into two independent eigenvalue problems, posed on the even and odd subspaces. The problem on the odd subspace is in fact a trivial one (i.e., no non-trivial solutions). This can be seen from (IV.11), as \mathcal{H} restricted to the odd subspace is in fact a positive operator, i.e. $\mathcal{H}|_{X_{odd}} \geq 0$. Indeed, as ϕ, ψ are even functions

$$X_{odd} \perp \begin{pmatrix} -\phi'' + (4 - \omega^2)\phi \\ 0 \\ -\psi'' + (4 - 9\omega^2)\psi \\ 0 \end{pmatrix}.$$

and hence $\mathcal{H}|_{X_{odd}} \geq 0$. So, now we proceed to find the adjoint eigenvectors corresponding to the kernel vector $\begin{pmatrix} 0 \\ \phi \\ 0 \\ 3\psi \end{pmatrix}$.

We solve

$$\begin{pmatrix} 0 & -I \\ I & -\mathcal{J} \end{pmatrix} \begin{pmatrix} \mathcal{H} & 0 \\ 0 & I \end{pmatrix} \vec{\eta} = \begin{pmatrix} 0 \\ \phi \\ 0 \\ 3\psi \end{pmatrix}.$$

Applying the inverse operator $\begin{pmatrix} -\mathcal{J} & I \\ -I & 0 \end{pmatrix}$ we obtain for $\vec{\eta} = \begin{pmatrix} \eta_1 \\ \eta_2 \end{pmatrix}$,

$$\eta_2 = - \begin{pmatrix} 0 \\ \phi \\ 0 \\ 3\psi \end{pmatrix}, \mathcal{H}\eta_1 = -\mathcal{J} \begin{pmatrix} 0 \\ \phi \\ 0 \\ 3\psi \end{pmatrix} = 2\omega \begin{pmatrix} \phi \\ 0 \\ 9\psi \\ 0 \end{pmatrix}.$$

Taking derivative with respect to ω in the profile equation (II.5) leads to the formula

$$\mathcal{H}[\partial_\omega \begin{pmatrix} \phi \\ 0 \\ \psi \\ 0 \end{pmatrix}] = 2\omega \begin{pmatrix} \phi \\ 0 \\ 9\psi \\ 0 \end{pmatrix}. \quad (\text{V.1})$$

Thus, we can take

$$\eta_1 = \mathcal{H}^{-1}[2\omega \begin{pmatrix} \phi \\ 0 \\ 9\psi \\ 0 \end{pmatrix}] = \partial_\omega \begin{pmatrix} \phi \\ 0 \\ \psi \\ 0 \end{pmatrix}.$$

In this fashion, we have identified an element $\vec{\eta} = \begin{pmatrix} \eta_1 \\ \eta_2 \end{pmatrix}$ of the generalized kernel, namely

$$\eta_1 = \partial_\omega \begin{pmatrix} \phi \\ 0 \\ \psi \\ 0 \end{pmatrix}, \quad \eta_2 = - \begin{pmatrix} 0 \\ \phi \\ 0 \\ 3\psi \end{pmatrix}.$$

Proceeding to find further elements of $gKer$, we need to solve

$$\begin{pmatrix} 0 & -I \\ I & -\mathcal{J} \end{pmatrix} \begin{pmatrix} \mathcal{H} & 0 \\ 0 & I \end{pmatrix} \vec{z} = \vec{\eta}$$

Applying again the inverse, we are led to the following system

$$\mathcal{H}z_1 = -\mathcal{J}\eta_1 + \eta_2, \quad z_2 = -\eta_1.$$

This of course requires a solvability condition in the first component, namely

$$-\mathcal{J}\eta_1 + \eta_2 \perp Ker[\mathcal{H}] = span \left[\begin{pmatrix} 0 \\ \phi \\ 0 \\ 3\psi \end{pmatrix} \right]. \quad (\text{V.2})$$

Equivalently, the second adjoint eigenvector \vec{z} does not exist, whenever the solvability condition (V.2) is violated. More precisely,

$$0 \neq \langle -\mathcal{J}\eta_1 + \eta_2, \begin{pmatrix} 0 \\ \phi \\ 0 \\ 3\psi \end{pmatrix} \rangle = - \left(\omega \partial_\omega \left(\int \phi^2 + 9\psi^2 \right) + \int \phi^2 + 9\psi^2 \right) \quad (\text{V.3})$$

Under the condition (V.3), we have that $dim(gKer) = 1$, and hence the matrix $D \in \mathcal{M}_{1 \times 1}$, with

$$\mathcal{D}_{11} = \langle \begin{pmatrix} \mathcal{H} & 0 \\ 0 & I \end{pmatrix} \vec{\eta}, \vec{\eta} \rangle = \langle \mathcal{H}\eta_1, \eta_1 \rangle + \langle \eta_2, \eta_2 \rangle = \omega \partial_\omega \int_{\mathbb{R}} (\phi^2 + 9\psi^2) dx + \int_{\mathbb{R}} (\phi^2 + 9\psi^2) dx$$

Thus, according to the index counting theory, more precisely (III.4), the waves are stable in the case of $n(L) = 1$, if and only if

$$\partial_\omega \left(\omega \int_{\mathbb{R}} (\phi^2 + 9\psi^2) dx \right) = \omega \partial_\omega \int_{\mathbb{R}} (\phi^2 + 9\psi^2) dx + \int_{\mathbb{R}} (\phi^2 + 9\psi^2) dx < 0 \quad (\text{V.4})$$

Equivalently, in this case, the stability is equivalent to the property that

$$\omega \rightarrow \omega \int_{\mathbb{R}} (\phi^2 + 9\psi^2) dx$$

is a decreasing function.

In what follows, we will explore the different branches of the real solutions of Eqs. (II.5), which can be used according to the prescription of Eq. (II.3) in order to develop approximations to the oscillon periodic orbits of Eq. (II.1). We will subsequently study the stability of these states at the level of the reduced equations (II.4) and will then seek to connect the resulting conclusions with the original PDE of Eq. (II.1).

VI. NUMERICAL RESULTS

In our efforts to identify solutions to Eqs. (II.5), we identified 3 branches of possible solutions. We thus hereafter explore these solution branches that can be discerned in the diagram of the left panel of Fig. 1. This is complemented by an example of the profile of each of the oscillon branches that we have identified in the right panel of the figure. The former represents the amplitude of the $\phi(x)$ component, providing accordingly a useful bifurcation diagnostic. The first branch of solutions, depicted in blue, corresponds to $(0, +)$ oscillons, i.e., $\phi(x) = 0, \psi(x) > 0$, with only the third harmonic being present. These waveforms have been found to exist for any $\omega \in (0, 2/3)$, which is in line with earlier dynamical observations of the original PDE of Eq. (II.1) [17]. In the latter the frequency of these waves $3\omega < 2 \Rightarrow \omega < 2/3$. [27] On the other hand, the red line in Fig. 1 corresponds to solutions of the $(-, +)$ form, i.e. $\phi(x) < 0, \psi(x) > 0$, in the interval $\omega \in (0, \omega_0)$ with $\omega_0 = 0.5242$; as one can see, the amplitude of the ϕ component tends to zero when $\omega \rightarrow \omega_0$ and becomes zero just at $\omega = \omega_0$. For $\omega > \omega_0$, $\phi(x) > 0$ and $\psi(x) > 0$, meaning that the solution, in our notation, becomes of the $(+, +)$ form, until the solution disappears for only slightly larger frequency, i.e., at $\omega = \omega_+ = 0.5323$ through a saddle-center bifurcation with a third branch, also of the $(+, +)$ form and depicted in black. In particular, the branch depicted with a black line has a larger (positive) amplitude within its ϕ component, while the red one has a lower amplitude and the two collide and disappear hand-in-hand at $\omega = \omega_+ = 0.5323$. However, this saddle-center event is not the only bifurcation occurring. As the $(-, +)$ branch turns to a $(+, +)$ one with $\phi(x)$ crossing through 0, this red branch “collides” in a transcritical-like bifurcation with symmetry, as we will see below, with the blue branch of the form $(0, +)$. We will explore the implications of these bifurcations for the branches involved in what follows.

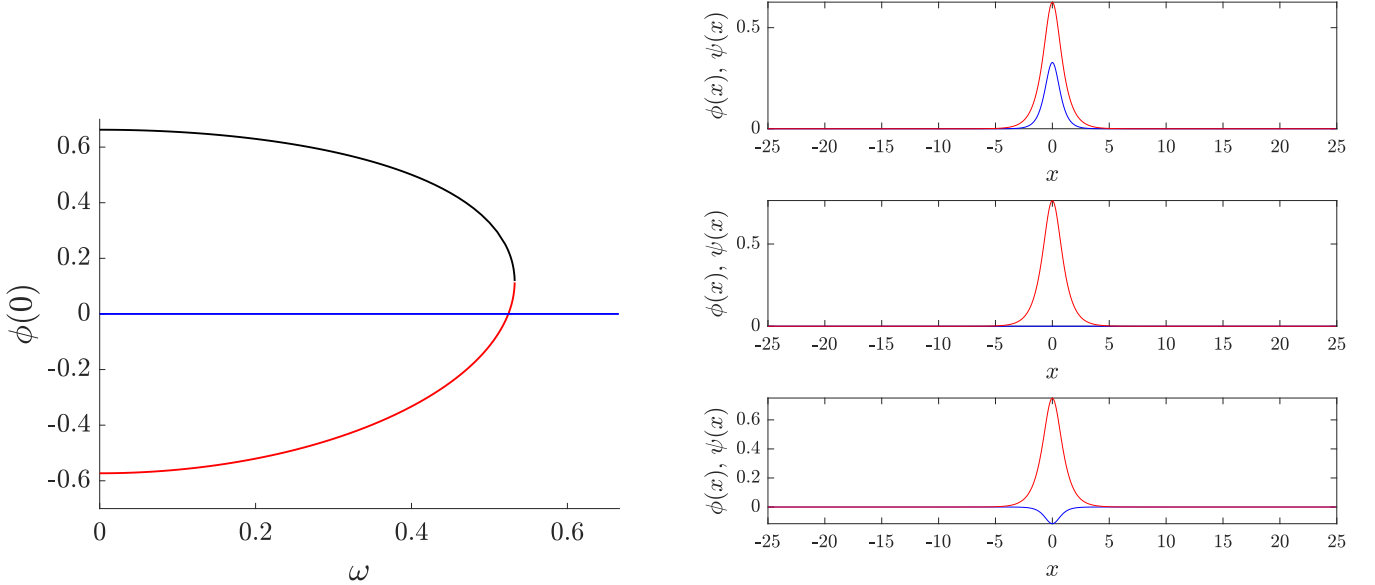


FIG. 1. (Left panel) A bifurcation diagram of the solutions to Eq. (II.5) that were identified in our analysis. The value of the first component at $x = 0$ ($\phi(0)$) is used as a bifurcation diagnostic. The blue solid line represents a $(0, +)$ branch with only the third harmonic being “populated”. The black branch is a $(+, +)$ branch with both components featuring a positive (sign-definite) waveform. Finally, the red branch is a $(-, +)$ branch with the two components starting with opposite values, but the first component crosses $\phi(x) = 0$ when $\omega \rightarrow \omega_0 = 0.5242$ leading to both components becoming positive before this branch collides in a saddle-center bifurcation with the other $(+, +)$ branch at $\omega = \omega_+ = 0.5323$. (Right panel) Profiles of the oscillons for the different branches (from top to bottom: $(+, +)$, $(0, +)$ and $(-, +)$ branches) at $\omega = 0.5$. Blue (red) curves correspond to the $\phi(x)$ ($\psi(x)$) component.

In Fig. 2 we show the dependence with ω of the VK-like quantity discussed earlier, namely $\omega \int_{\mathbb{R}} (\phi^2 + 9\psi^2) dx$. We observe a maximum of the $(0, +)$ oscillon of the blue branch at $\omega = 0.4719$ and another one for the $(-, +)$ oscillon of the red branch at $\omega = 0.5200$. Interestingly, for the blue branch, we will see that the change of monotonicity of the relevant quantity is associated with a real eigenvalue changing to imaginary, as the relevant quantity changes from increasing to decreasing. On the other hand, for the black $(+, +)$ branch, the “wrong” monotonicity (i.e., its increasing nature) implies that this branch will always feature real eigenvalue pairs, as we will see to be the case in what follows. Interestingly, the situation for the red branch will be seen in our eigenvalue analysis to be more

complicated.

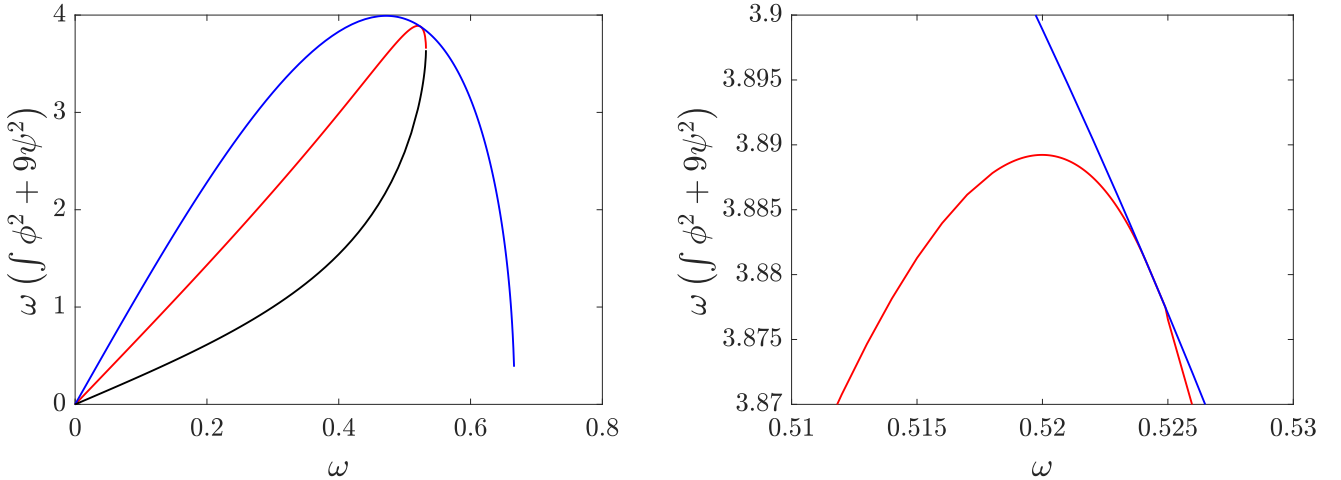


FIG. 2. In this figure, we demonstrate the $\omega \int_{\mathbb{R}} (\phi^2 + 9\psi^2) dx$ quantity that we associated in Theorem II.4 with stability. The red $(-, +)$ branch changes monotonicity (and hence stability) at $\omega = 0.52$; see also the zoom-in of the right panel. The black $(+, +)$ branch is always increasing and hence always bears real eigenvalues. The blue $(0, +)$ branch has a change of monotonicity at $\omega = 0.4719$ analyzed further below.

Another quantity that was deemed central to our theoretical analysis of Section IV, when constructing the waves was the functional J/I^2 where J and I are defined in Proposition IV.1. Accordingly, in Fig. 3, we illustrate the quantity J/I^2 versus ω . One can see that the largest value of the relevant quantity pertains to the black $(+, +)$ branch for $\omega < 0.5316$, when the blue branch acquires the largest J/I^2 value and becomes the global maximizer until the branch ceases to exist at $\omega = 2/3$. The relevant global maximizer is unstable throughout its existence (irrespectively of whether it pertains to the black or blue branch), as we will confirm in our eigenvalue analysis.

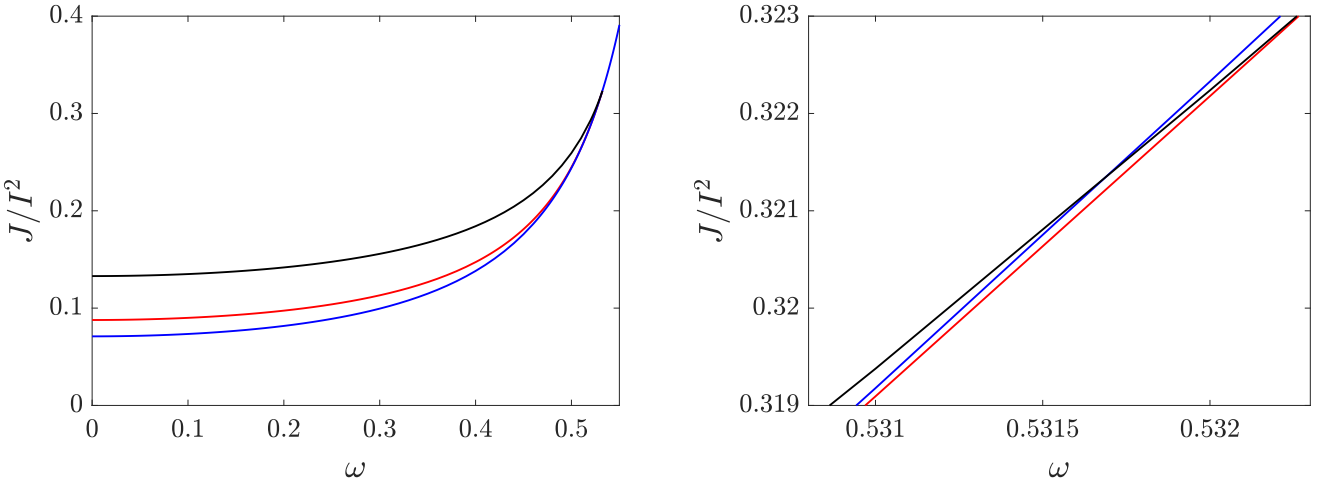


FIG. 3. The quantity J/I^2 where J and I are defined in Proposition IV.1 is given on the left panel for each of the previously discussed branches. The right panel is again a zoom-in where a crossing of this quantity for the black and blue branch takes place at $\omega < 0.5316$.

We now turn to an analysis of the eigenvalues of the different branches to help elucidate their stability and connect them to the VK-criterion discussed in Theorem II.4. As discussed already above, and in line with the VK criterion of the Theorem, the $(+, +)$ branch is always unstable because of a real eigenvalue pair. Fig. 4 shows the relevant real part of the (maximal) eigenvalue of the linearization around such solutions. A typical example of the relevant solution and its spectral place is shown in Fig. 5.

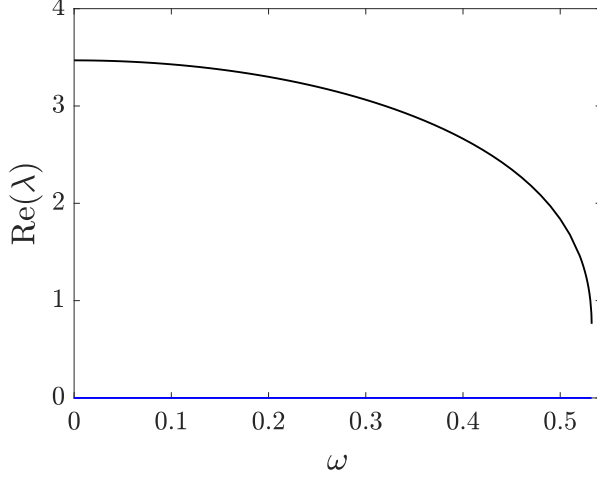


FIG. 4. Dependence of the real part of the eigenvalues of the $(+, +)$ family with respect to the frequency. The black line indicates that such a real eigenvalue exists for all the frequencies for which the branch exists, thus rendering it spectrally unstable.

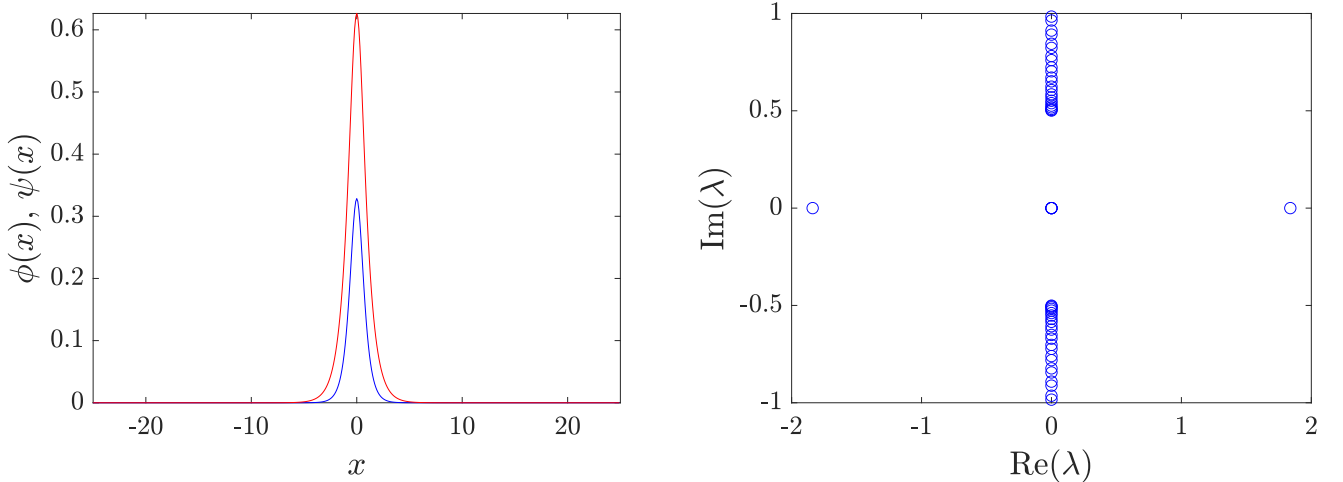


FIG. 5. Oscillation in the $(+, +)$ branch with $\omega = 0.5$ (left panel) and the corresponding spectral plane featuring a real (unstable) eigenvalue.

From the representation of the real and imaginary parts of the spectrum for the $(0, +)$ solutions in Fig. 6, one can observe that such a solution is unstable for $\omega < 0.5121$, as at such a value of the frequency parameter, there is a Hopf bifurcation where a quartet of complex eigenvalues becomes imaginary, while at $\omega = 0.4719$, a real eigenvalue pair becomes imaginary; in addition, at $\omega = \omega_0 \equiv 0.5242$ there is an eigenvalue that becomes zero although it is imaginary past this value. This is fairly remarkable as what happens here is that the positive and negative imaginary parts of the eigenvalue “exchange sides” (i.e., the positive becomes negative and vice versa) *without* the state changing its stability at the transcritical-like point ω_0 . We will use here the term “transcritical-like”, since in a regular transcritical bifurcation, the two branches exist both before and after their collision (where they become identical), yet they exchange stability at the critical point. Here, the branches involved collide (meaning that they exist before and after the critical point and coincide at that point), yet due to each of them involving a pair of eigenvalues, their stability is not exchanged; rather the relevant eigenvalue pairs switch sides (positives become negatives and vice versa, for real eigenvalues in one of the branches and imaginary ones in the other).

Importantly, it is relevant to note that these results are semi-quantitatively in line with the findings of [17] at the level of the full original PDE of Eq. (II.1), as the latter findings suggest that the single frequency waveform is dynamically robust for $\sqrt{2}/3 \equiv 0.4714 < \omega < 2/3$ in our notation. We indeed identify an eigenvalue transition at

0.4719 (from real to imaginary) very close to the above threshold, while the complete stabilization of this steady state (when it becomes devoid of Hamiltonian Hopf bifurcations) occurs at $\omega = 0.5121$. Some typical examples of the corresponding the $(0, +)$ solution branch spectral planes are shown in Fig. 7.

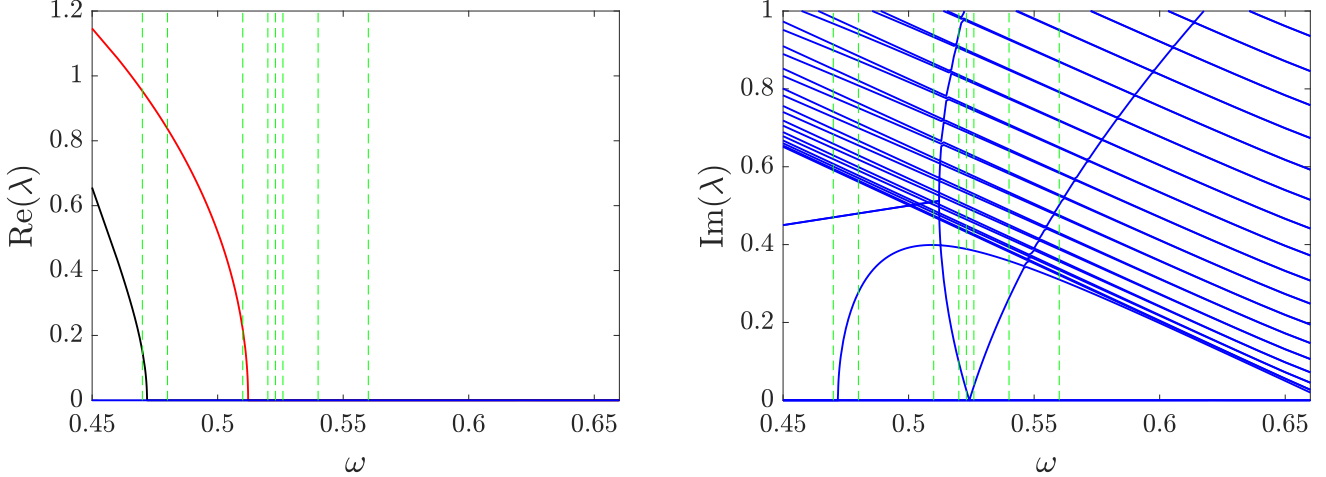


FIG. 6. Dependence of the real (left panel) and imaginary (right panel) parts of the eigenvalues of the $(0, +)$ family with respect to the frequency ω . A black line indicates that an eigenvalue is real and red lines are associated with eigenvalues with non-zero imaginary part, i.e., complex ones. Vertical lines correspond to the values of ω for which the spectral plane is represented in Fig. 7. Notice that the solution is fully spectrally stable for $\omega > 0.5121$.

Finally, as can be deduced from Fig. 8, the $(-, +)$ solutions are unstable for $\omega < 0.5183$ as at such a value, the oscillon becomes stable via a Hopf bifurcation; i.e., a quartet turns into two imaginary pairs at this frequency. The relevant branch is stable for a very narrow frequency interval until $\omega = 0.5200$ where an eigenvalue pair turns from imaginary to real, leading to the subsequent destabilization of the branch. Notice that we have checked the latter to be consonant with the Hamiltonian-Krein index theory, given that for this branch $n(\mathcal{H}) = 2$, while upon change of monotonicity $n(\mathcal{D}) = 1$, hence per the relevant index theory [28], there should exist a real eigenvalue pair, which is what we observe.

As ω increases further, again very proximally in frequency, i.e., at $\omega = \omega_0 = 0.5242$, the collision of the $(-, +)$ and the $(0, +)$ branch discussed above takes place. However, importantly, this is a rather special example of a transcritical-like bifurcation *with symmetry*. That is to say, as we pointed out above, for the $(-, +)$ branch, the eigenvalues of the real pair exchange sides while both remain real. Accordingly, the $(-, +)$ branch before and after the bifurcation remains unstable, just like the $(0, +)$ branch with which it collides preserves its stability before and after the bifurcation. At the critical point for the $(-, +)$, the $\phi(x)$ component crosses through zero (from negative to positive, as the frequency increases).

The oscillons obtained through the solution of Eqs. (II.5) can be used as seeds for fixed point methods that allows to solve the original KG PDE of Eq. (II.1) in the form of periodic orbits (breathers) of the form

$$z(t, x) = 2 \sum_{k=1}^{\infty} y_k(x) \cos [(2k-1)\omega_b t] \quad (\text{VI.1})$$

The main drawback of working with breathers is that they do not exist in a genuinely infinite domain because of resonances of $k > 1$ harmonics with the linear modes band. However, in a finite domain, there can appear gaps in the spectrum that can be controlled by the size of the domain, whose inverse controls the discretization in wavenumbers (and accordingly in frequencies). Then, breathers whose harmonics lie in the resulting frequency gaps have a short interval of stability that is dependent of the domain size and the discretization parameter. In addition, the only oscillon family which gives rise to breathers with features similar to that of the original oscillon is that of the $(0, +)$ solutions above. Because of this, we have only considered breathers coming from the $(0, +)$ branch; in that case, the seed for the fixed point algorithm (Newton-Raphson) is taken as $y_1(x) = \psi(x)$ and $y_k(x) = 0$ for $k \geq 2$, and $\omega_b = 3\omega$. In this way, one can find breathers that can potentially be stable as we now discuss.

Based on the resulting solutions, we have considered the dynamics of the KG PDE by taking as initial condition $z(0, x)$ a breather with frequency 3ω , i.e., $z(0, x) = 2 \sum_k y_k(x)$ and comparing it with that stemming from an oscillon,

i.e. $z(0, x) = 2(\phi(x) + \psi(x))$. It is worthwhile to note that in all the relevant examples where the KG PDE is considered, per the form of the obtained breathers, the velocity initial condition $z_t(0, x)$ is set to zero; cf. also Eq. (VI.1). When considering the $(0, +)$ solution, naturally, $\phi(x) = 0$. Fig. 10 considers the dynamics when taking as initial condition an oscillon with $\omega = 0.45$ and comparing it with the evolution of a breather with frequency 3ω ; to this aim, a spatio-temporal diagram is shown together with the spectrum of the Floquet operator of the breather, from which one can see that the dominant instability is of exponential nature. The evolution of the central site and its Fourier spectrum shown also complements the picture that can be summarized as the emergence of a quasi-periodic breather-like structure that in the case of the initial breather is created after a transient. From the Fourier spectra one can see that the dominant frequency for the dynamics emerging from the oscillon (breather) is 1.031 (1.717) and a secondary peak of the spectrum is observed around 0.999 (1.665). Although the dynamics draws a number of parallels between the two cases, there are also some notable differences. In the approximate oscillon case generated by the steady state solution of II.5, we observe a continuously, yet very slowly decaying structure. On the other hand, the obtained numerically exact solution is indeed a periodic orbit, up to numerical tolerance error, yet this error suffices to eventually destabilize the originally genuinely periodic evolution for sufficiently long times. The resulting structures are similar in nature, albeit with different frequencies involved in the long term dynamics.

Figure 11 shows the outcome for the oscillon with $\omega = 0.5$ and the breather counterpart with frequency 3ω . In this case, the instabilities of the breather are very weak and its shape remains almost invariant for the long time evolutions of the order of 1000 time units reported. It is nevertheless relevant to point out that in this case too, the genuine breather solution is expected to be destabilized for sufficiently long times. Finally, in Fig. 12 one can observe that for $\omega = 0.61$, both the oscillon and the breather are stable, and the oscillon dynamics is quite similar to that of the breather. In addition, we observe the stability of the breather from its Floquet spectrum; in fact, in the bottom right panel of Fig. 12 one can see the dependence of the energy versus the breather frequency, and observe the existence of the typical ladders (“spikes”) caused by the resonance with phonons, i.e., with linear continuous spectrum modes. It is relevant to note here that in the context of oscillons, such a ladder structure has also been reported in the realm of a three-dimensional radial oscillon in a ball in the study of [29]. Interestingly, for $\omega_b \gtrsim 1.82$, the resonances are so small that they cannot be discerned and the breather is stable for that branch. Prior to the resonance at $\omega_b = 1.8199$, the breather solution is stable in the decreasing portion of the branch, while it is unstable in the (narrow) increasing portion evident in Fig. 12. While the presence of the continuous spectrum resonances renders the continuation of the relevant breather branch for all frequencies tricky, our expectation is that for $3\omega > \sqrt{2}$, the breather branch will have a character similar to what is reported above with a typical marginally stable Floquet spectrum (in the exception of small finite-size induced complex [20] multipliers). Nevertheless, near the resonances with each relevant phonon mode, there will be a portion of increasing energy-frequency dependence, corresponding to breather instability, in line with the corresponding stability criterion of [30].

Finally, we have also considered the dynamics of $(-, +)$ and $(+, +)$ oscillons. As mentioned above, we have been unable to systematically identify breathers pertaining to such steady state solutions, hence, instead, in what follows, we have focused on the initialization of the original KG PDE of Eq. (II.1) with the solution of the steady state problem of Eqs. (II.5). In the case of $(-, +)$ (see Fig. 13) we have observed that the oscillon generically disperses although it still oscillates as one can see from the panels showing $z(t, 0)$; when the frequency increases, the breather dispersion decreases and, if the growth rate is small enough, a robust quasi-periodic breather-like excitation is generated. As an example, one can observe that for the $(-, +)$ oscillon with $\omega = 0.515$, resulting in a quasi-periodic breather with dominant frequency 1.684 and secondary frequency 1.370. For the $(+, +)$ oscillons, the dynamics typically lead to blow up, as one can see in the left panel of Fig. 14 (cf. with the right panel of the figure stemming from the $(-, +)$ branch which leads again to quasi-periodic dynamics).

VII. CONCLUSIONS AND FUTURE CHALLENGES

In the present work we have revisited the study of oscillons in one spatial and one temporal dimension in the class of “flipped sign” ϕ^4 models in the spirit of the work of [15]. Motivated by the recent developments in the work of [17, 18], we have provided an alternative mathematical approach towards the study of these oscillons, which, however, we have argued extends well past this particular PDE. We have reduced the problem into effectively a two-mode system, concerning the dynamics of the first and third harmonic (given the nature of the cubic nonlinearity). The steady states of the resulting PDE system provide a starting point approximation towards the identification of the full time-periodic oscillon states of the original model. Here we have provided a mathematical analysis, using the tools of index theory, of dynamical systems (through the use of suitable Lyapunov type functionals) and of nonlinear PDEs, developing quantities whose monotonicity change is tantamount to the change of the steady state’s stability. We have then identified the resulting states numerically and confirmed our stability conclusions, as well as provided a detailed numerical bifurcation analysis of such states, bearing numerous unusual features. These included, e.g., a

transcritical-like bifurcation with symmetry but also other bifurcations (such as saddle-centers) between some of the relevant stationary states. Finally, we have compared these findings with the full PDE model finding good agreement between the existence and stability of one of the branches and the corresponding PDE features. Other of the branches involved significant contributions of higher harmonics and thus led to less meaningful results at the level of full oscillons, although they involved a considerable level of mathematical interest in their reduced model analysis.

We believe that this approach sheds light on a mathematical technique that can be more widely used for periodic solutions in continuum (but possibly also in discrete) problems. Arguably, the resulting reduced PDE models and their steady states are of interest in their own right, yet it seems relevant to establish conditions under which the latter are more closely connected to the original problem and its time-periodic waveforms. In that spirit, such a technique could be used also for the higher-dimensional study and analysis of oscillons that is of wide relevance to cosmological problems [1]. Such studies, both discrete and higher dimensional of such time-periodic and potentially oscillon-type solutions are currently under consideration and will be reported in future publications.

Conflict of interest statement: The authors declare that they have no competing financial interests or personal relationships that could have influenced the work reported in this paper.

Data availability statement: The data that support the findings of this study are mostly contained in the paper. Additional datasets can be made available from the corresponding author upon request.

Acknowledgements: We are grateful to Professor Igor Barashenkov for bringing this important problem to our attention, as well as for numerous constructive remarks on this work. This material is based upon work supported by the U.S. National Science Foundation under the awards PHY-2110030, PHY-2408988, DMS-2204702 (PGK). J.C.-M. acknowledges support from the EU (ERDF program) through MICIU/AEI/10.13039/501100011033 under the project PID2022-143120OB-I00

[1] M. Gleiser, International Journal of Modern Physics D **16**, 219 (2007), <https://doi.org/10.1142/S0218271807009954>.

[2] X.-X. Kou, C. Tian, and S.-Y. Zhou, Classical and Quantum Gravity **38**, 045005 (2020).

[3] S. Antusch, F. Cefalà, S. Krippendorf, F. Muia, S. Orani, and F. Quevedo, Journal of High Energy Physics **2018**, 83 (2018).

[4] N. Graham, Phys. Rev. Lett. **98**, 101801 (2007).

[5] N. Graham, Phys. Rev. D **76**, 085017 (2007).

[6] V. Achilleos, F. K. Diakonos, D. J. Frantzeskakis, G. C. Katsimiga, X. N. Maintas, E. Manousakis, C. E. Tsagkarakis, and A. Tsapalis, Phys. Rev. D **88**, 045015 (2013).

[7] M. Gleiser and J. Thorarinson, Phys. Rev. D **76**, 041701 (2007).

[8] R. Rajaraman, *Solitons and Instantons: An Introduction to Solitons and Instantons in Quantum Field Theory* (North-Holland, Amsterdam, 1982).

[9] N. Manton and P. Sutcliffe, *Topological Solitons* (Cambridge University Press, Cambridge, England, 2004).

[10] E. J. Weinberg, *Classical Solutions in Quantum Field Theory: Solitons and Instantons in High Energy Physics* (Cambridge University Press, Cambridge, England, 2012).

[11] A. Vilenkin and E. P. S. Shellard, *Cosmic Strings and Other Topological Defects* (Cambridge University Press, Cambridge, England, 1994).

[12] E. Clément, L. Vanel, J. Rajchenbach, and J. Duran, Phys. Rev. E **53**, 2972 (1996).

[13] P. B. Umbanhowar, F. Melo, and H. L. Swinney, Nature **382**, 793 (1996), published 29 August 1996.

[14] E. J. Copeland, M. Gleiser, and H.-R. Müller, Phys. Rev. D **52**, 1920 (1995).

[15] A. M. Kosevich and A. S. Kovalev, Soviet Phys. JETP **40**, 891 (1975), received March 27, 1974.

[16] V. Achilleos, A. Álvarez, J. Cuevas, D. Frantzeskakis, N. Karachalios, P. Kevrekidis, and B. Sánchez-Rey, Physica D: Nonlinear Phenomena **244**, 1 (2013).

[17] I. V. Barashenkov and N. V. Alexeeva, Phys. Rev. D **108**, 096022 (2023).

[18] N. V. Alexeeva, I. V. Barashenkov, A. Dika, and R. D. Sousa, J. High Energy Phys. **2024** (10), 136, arXiv:2404.01028 [hep-th].

[19] S. Flach and A. V. Gorbach, Phys. Rep. **467**, 1 (2008).

[20] S. Aubry, Physica D **216**, 1 (2006).

[21] N. G. Vakhitov and A. A. Kolokolov, Radiophys. Quantum Electron. **16**, 783 (1973).

[22] But not necessarily real-valued, as this property was enforced with the ansatz (II.3).

[23] Positive, even and decreasing on $(0, +\infty)$.

[24] Note that the identity operators in the following formula act $Id : \mathbf{C}^4 \rightarrow \mathbf{C}^4$.

[25] Z. Lin and C. Zeng, Mem. Amer. Math. Soc. **1347**.

[26] The particular formulas were actually displayed before, but they become irrelevant here, due to (IV.7).

[27] It is important to highlight here that this is the branch analogous to the solutions presented in [17], as there are no solutions of the form $(+, 0)$ that are possible in model of Eqs. (II.5).

[28] T. Kapitula and K. Promislow, *Spectral and Dynamical Stability of Nonlinear Waves*, Applied Mathematical Sciences, Vol.

185 (Springer Science & Business Media, New York, 2013).

[29] N. V. Alexeeva, I. V. Barashenkov, A. A. Bogolubskaya, and E. V. Zemlyanaya, Phys. Rev. D **107**, 076023 (2023).

[30] P. G. Kevrekidis, J. Cuevas-Maraver, and D. E. Pelinovsky, Phys. Rev. Lett. **117**, 094101 (2016).

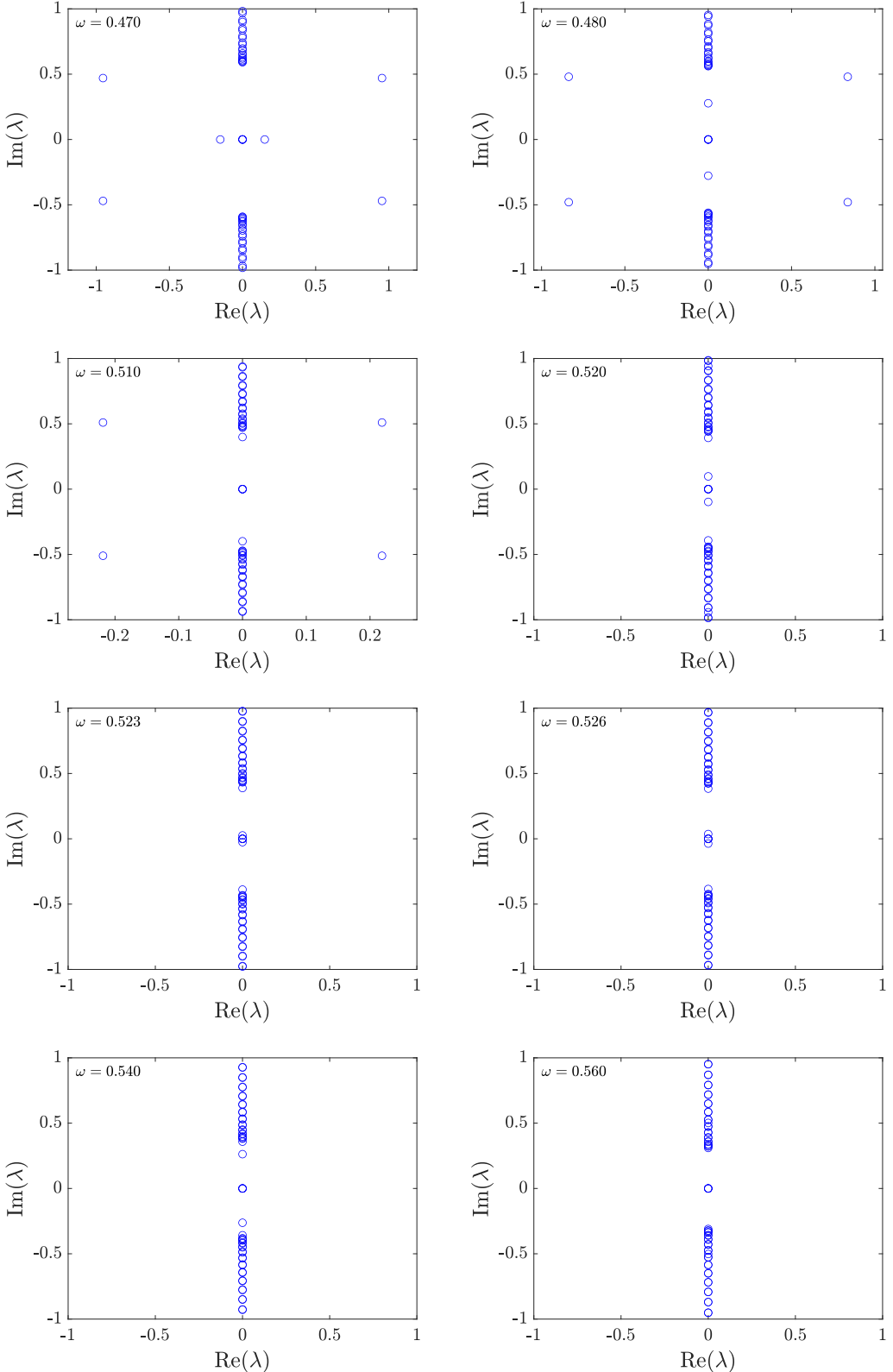


FIG. 7. Oscillons in the $(0, +)$ branch whose frequency corresponds to the green lines in Fig. 6. Each value of the frequency is displayed at the corresponding panel.

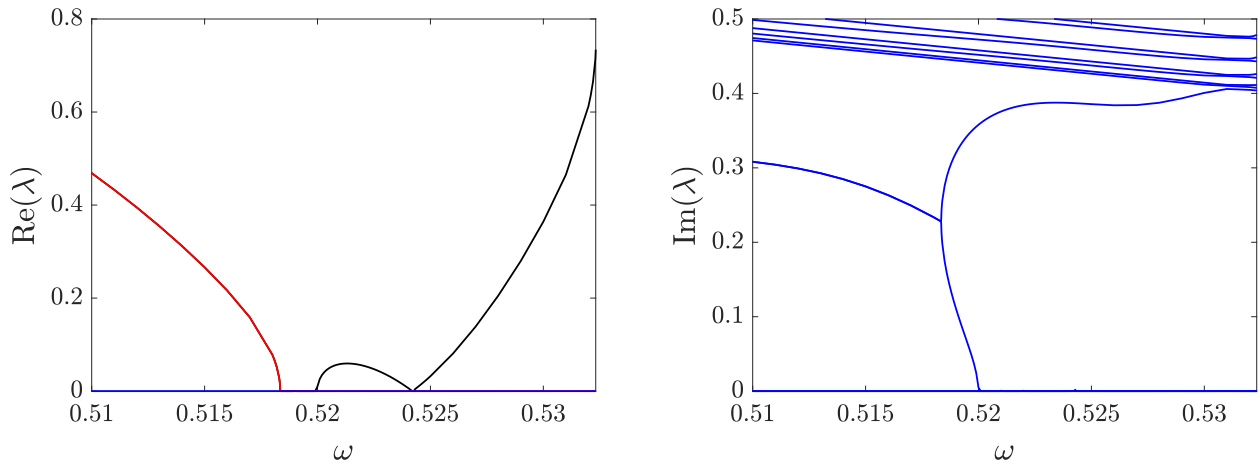


FIG. 8. Dependence of the real (left panel) and imaginary (right panel) parts of the eigenvalues of the $(-, +)$ family on the frequency. The black line indicates a real eigenvalue, while the red lines correspond to eigenvalues with nonzero imaginary part.

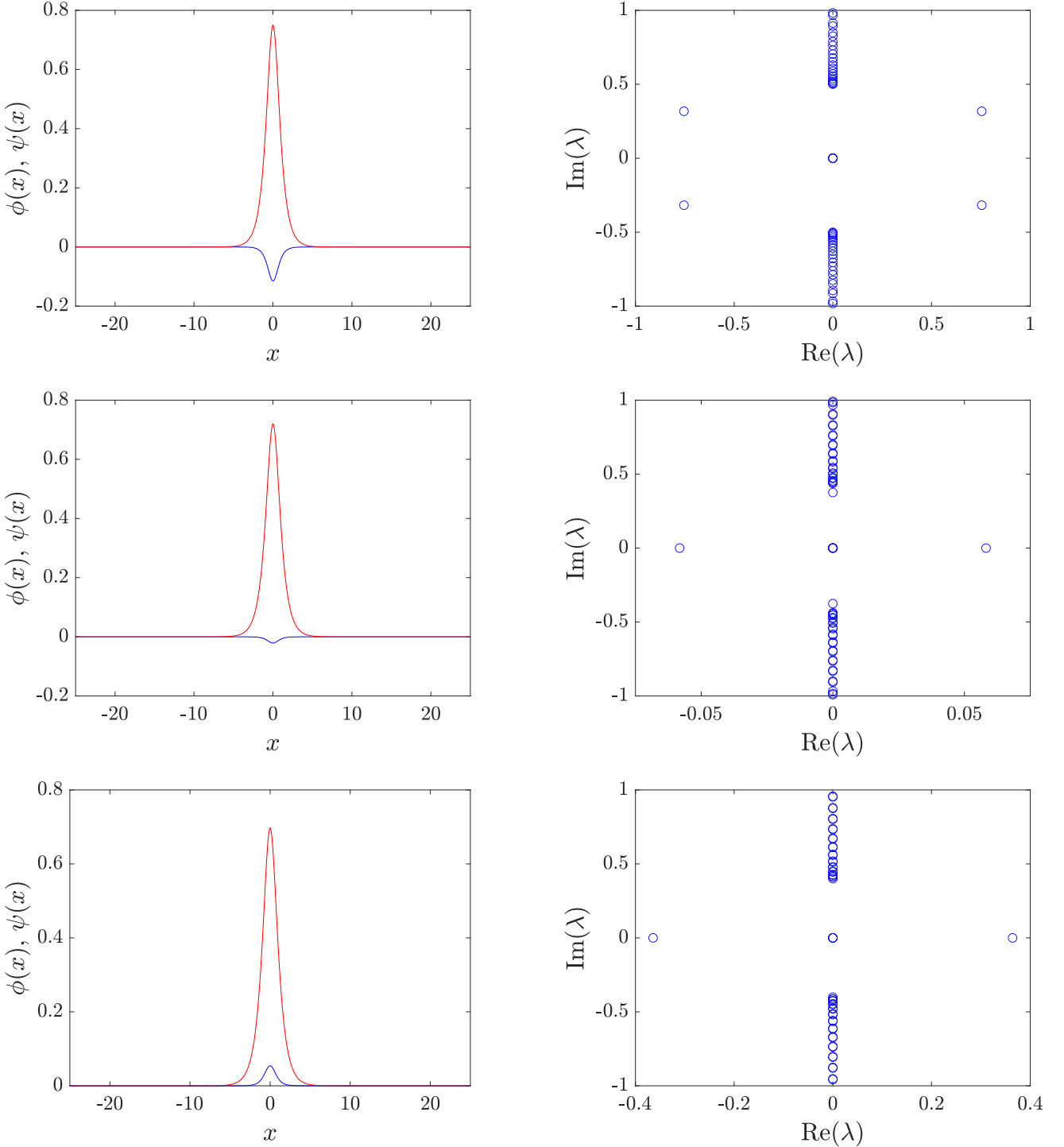


FIG. 9. Oscillons in the $(-, +)$ branch with $\omega = 0.5$ (top panels), $\omega = 0.521$ (middle panels), and $\omega = 0.53$ (bottom panels). The left panels show the solution profile, while the right ones show the corresponding spectral plane associated with the branch's stability.

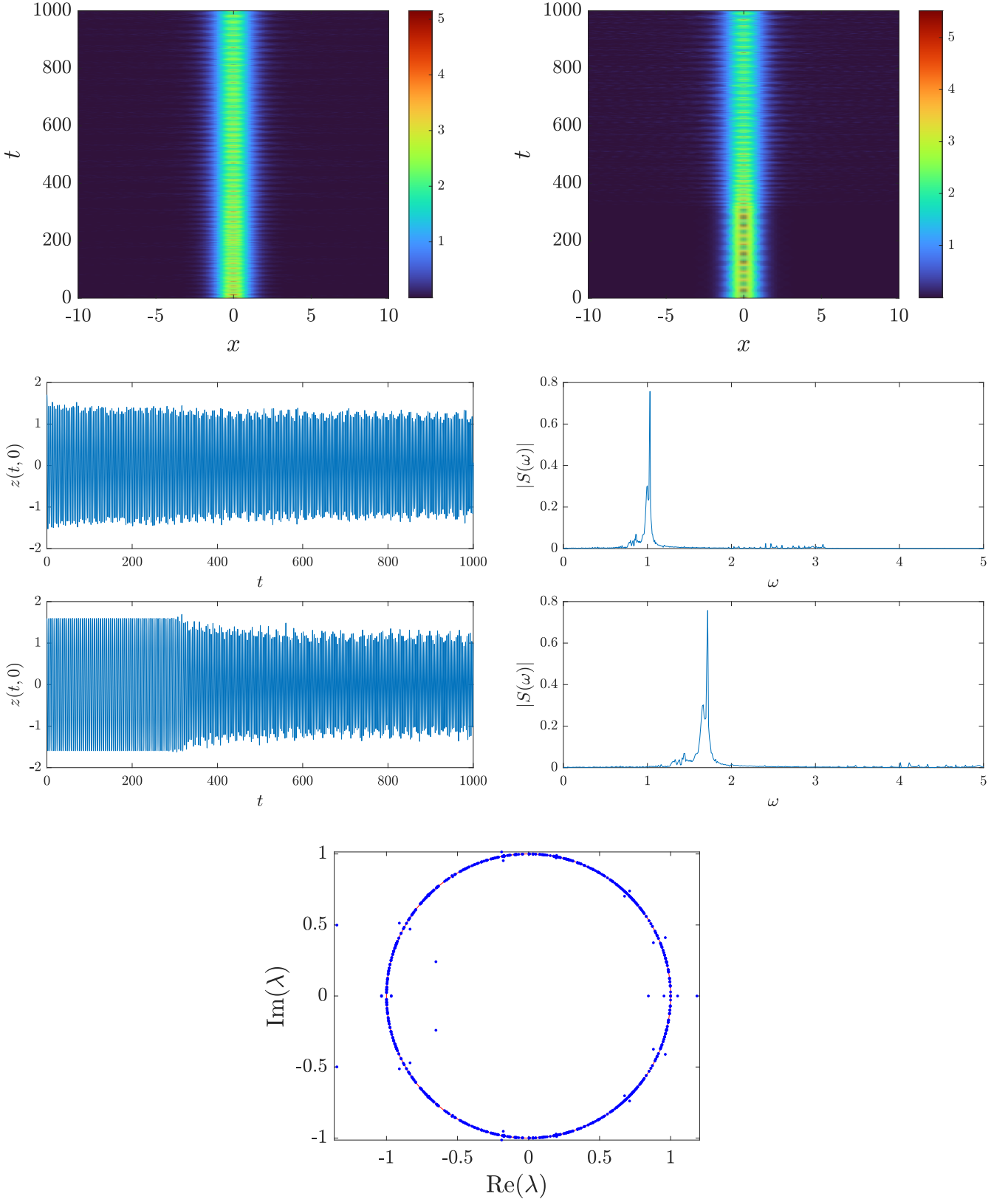


FIG. 10. (Top panels) Spatio-temporal evolution of the energy density for the KG equation using as initial condition a $(0, +)$ oscillon with frequency $\omega = 0.45$ (left) and a (genuinely time-periodic) breather with frequency 3ω (right). The middle panels show the time evolution of the central site and also its Fourier spectrum; top subpanels correspond to the oscillon, and bottom ones to the breather. The bottom panel displays the Floquet spectrum of the breather.

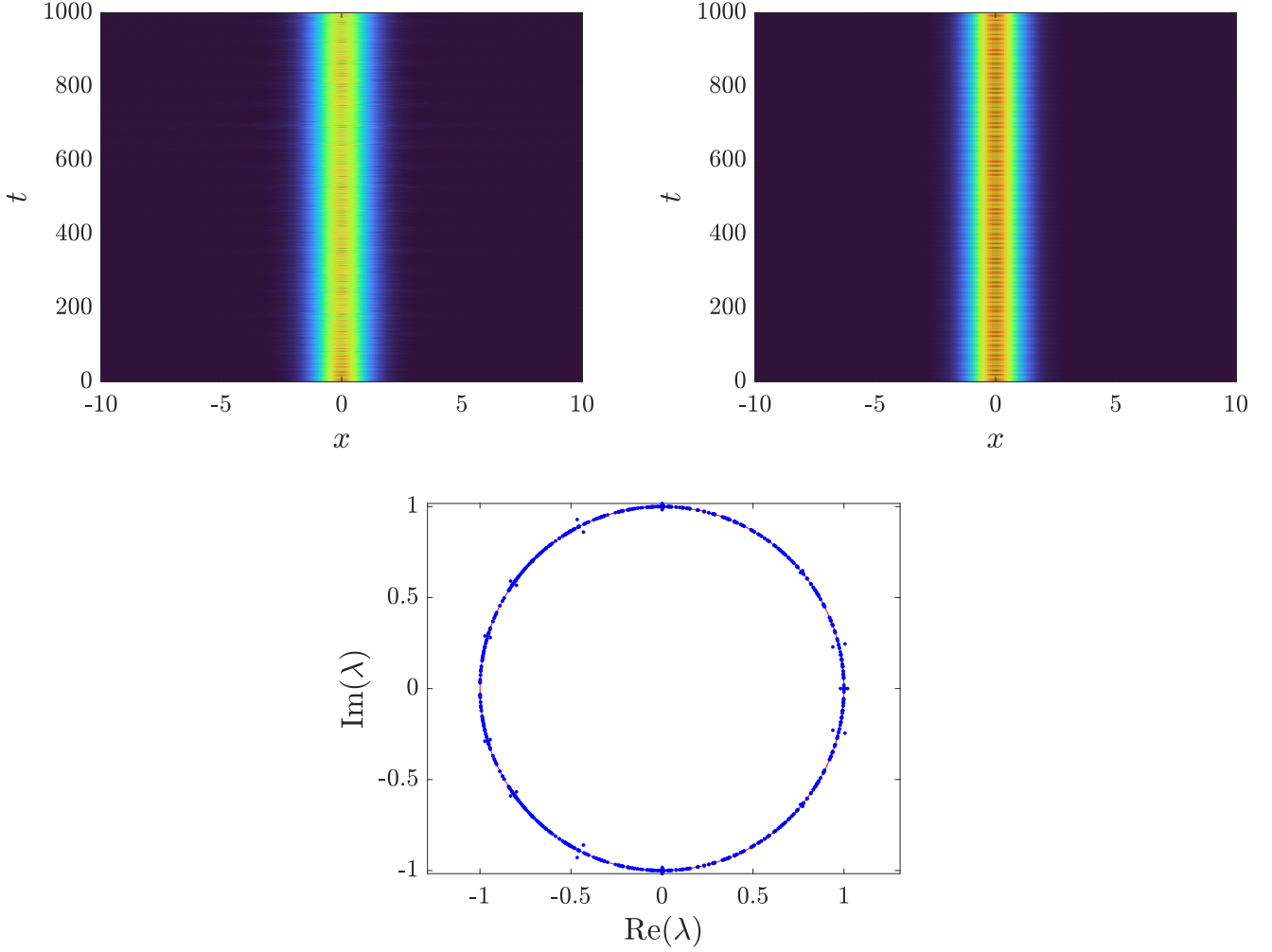


FIG. 11. Spatio-temporal evolution of the energy density for the KG equation using as initial condition a $(0, +)$ oscillon with frequency $\omega = 0.5$ (left panel) and a breather with frequency 3ω . The bottom panel displays the Floquet spectrum of the breather.

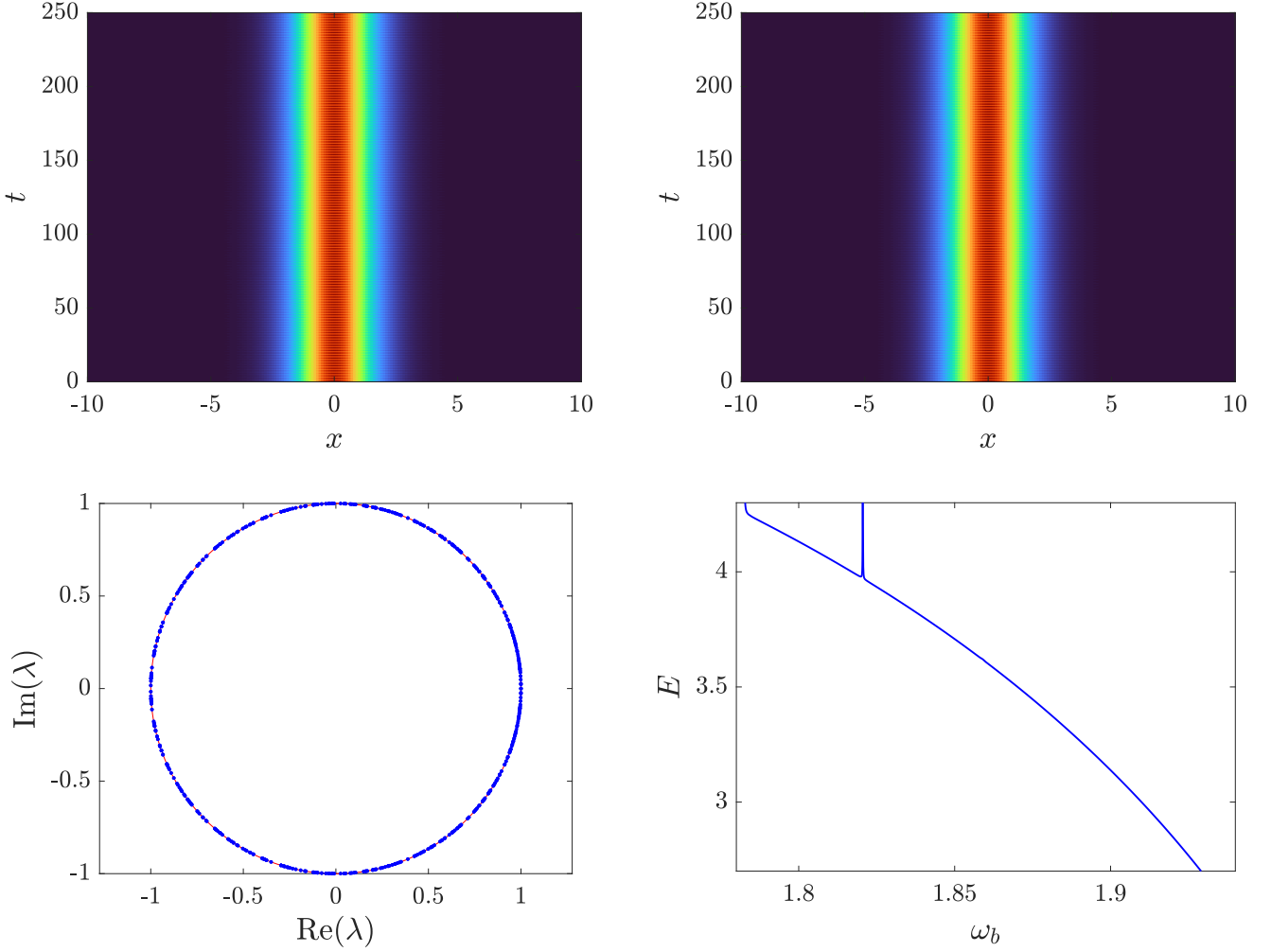


FIG. 12. Spatio-temporal evolution of the energy density for the KG equation using as initial condition a $(0, +)$ oscillon with frequency $\omega = 0.61$ (left panel) and a breather with frequency $\omega_b = 3\omega = 1.83$. The bottom left panel displays the Floquet spectrum of the breather and the bottom right panel shows the dependence of the energy versus the breather frequency for values of ω_b near 1.83.

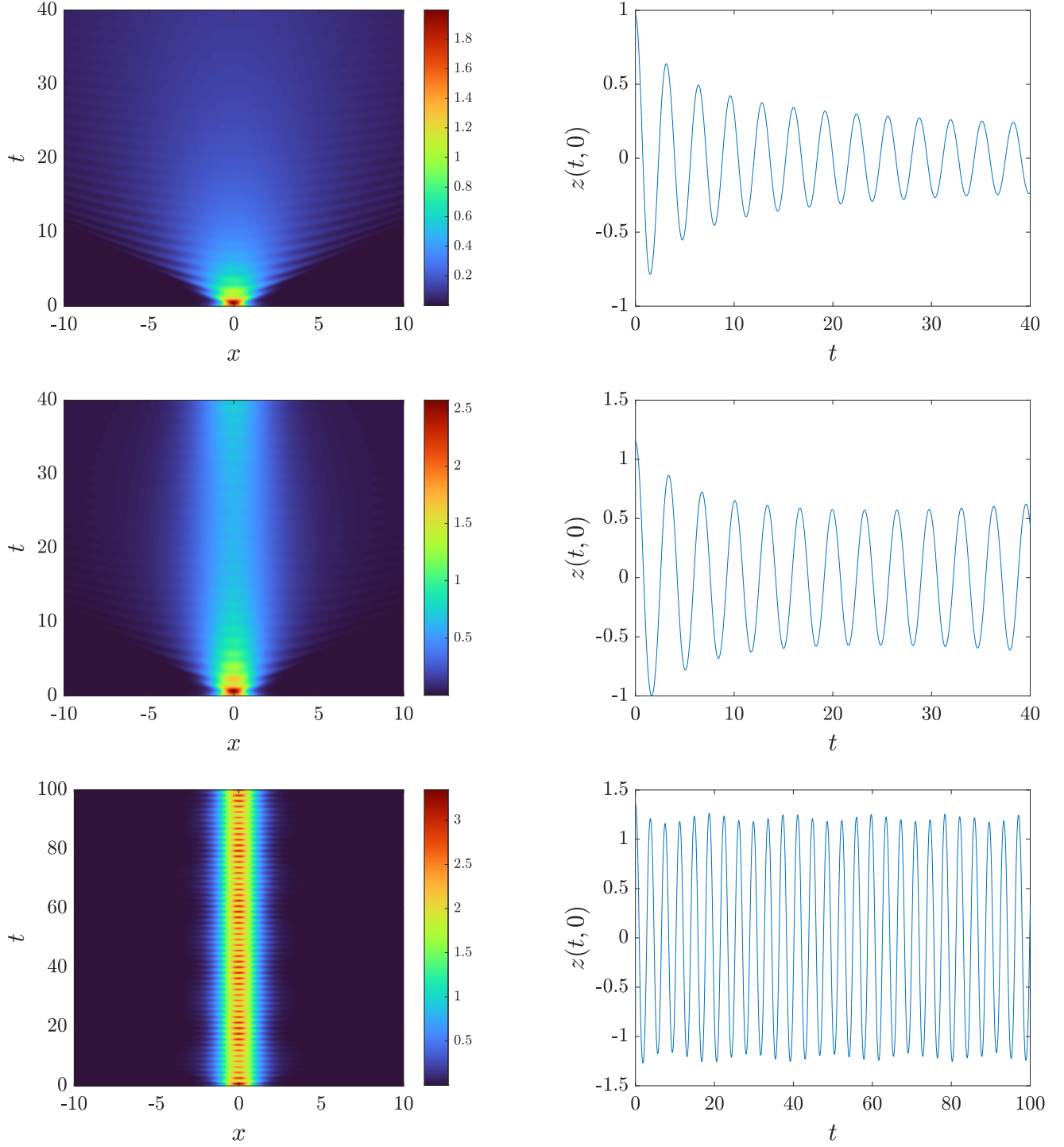


FIG. 13. (Left panels) Spatio-temporal evolution of the energy density for the KG equation using as initial condition a $(-, +)$ oscillon with frequency $\omega = 0.4$ (top panels), $\omega = 0.47$ (middle panels), and $\omega = 0.515$ (bottom panels). The right panels show the evolution for $z(t, 0)$, i.e., at $x = 0$, for the cases in the left panels.

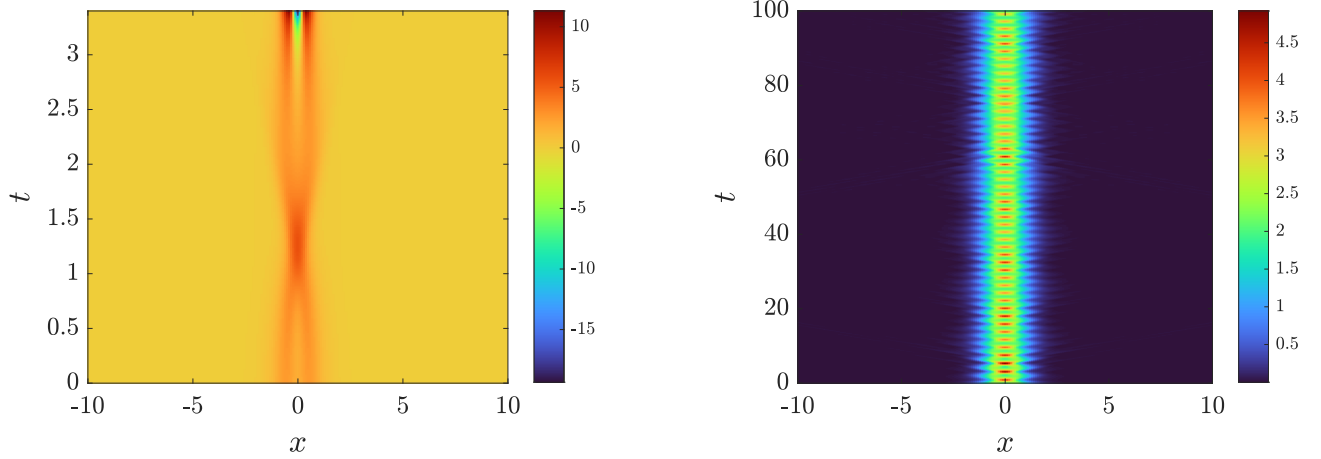


FIG. 14. Spatio-temporal evolution of the energy density for the KG equation using as initial condition a $(+, +)$ and a $(-, +)$ oscillon with frequency $\omega = 0.53$. Left (right) panel corresponds to the case when the initial condition is taken from the black (red) curve of Fig. 1.